

Scale invariant Green-Kubo relation for time averaged diffusivity

Philipp Meyer,¹ Eli Barkai,² and Holger Kantz¹

¹*Max Planck Institute for the Physics of Complex Systems Noethnitzer Str. 38 D 01187 Dresden Germany*

²*Department of Physics, Institute of Nanotechnology and Advanced Materials, Bar-Ilan University, Ramat-Gan, 52900, Israel*
(Dated: July 16, 2018)

In recent years it was shown both theoretically and experimentally that in certain systems exhibiting anomalous diffusion the time and ensemble average mean squared displacement are remarkably different. The ensemble average diffusivity is obtained from a scaling Green-Kubo relation, which connects the scale invariant non-stationary velocity correlation function with the transport coefficient. Here we obtain the relation between time averaged diffusivity, usually recorded in single particle tracking experiments, and the underlying scale invariant velocity correlation function. The time averaged mean squared displacement is given by $\overline{\delta^2} \sim 2D_\nu t^\beta \Delta^{\nu-\beta}$ where t is the total measurement time and Δ the lag time. Here $\nu > 1$ is the anomalous diffusion exponent obtained from ensemble averaged measurements $\langle x^2 \rangle \sim t^\nu$ while $\beta \geq -1$ marks the growth or decline of the kinetic energy $\langle v^2 \rangle \sim t^\beta$. Thus we establish a connection between exponents which can be read off the asymptotic properties of the velocity correlation function and similarly for the transport constant D_ν . We demonstrate our results with non-stationary scale invariant stochastic and deterministic models, thereby highlighting that systems with equivalent behavior in the ensemble average can differ strongly in their time average. This is the case, for example, if averaged kinetic energy is finite, i.e. $\beta = 0$, where $\langle \delta^2 \rangle \neq \langle x^2 \rangle$.

I. INTRODUCTION

A central result of nonequilibrium statistical physics is the Green-Kubo formalism. It relates the diffusion constant D of a normal diffusive system to the stationary velocity correlation function $\langle v(t + \tau)v(t) \rangle$ of the process. The brackets $\langle \dots \rangle$ denote the ensemble average. The Green-Kubo relation reads [1]

$$D = \int_0^\infty d\tau \langle v(t + \tau)v(t) \rangle, \quad (1)$$

where $v = dx/dt$. In theoretical physics we mostly consider ensemble averages while in the real world it is sometimes not possible to measure an ensemble because only one realization of a process is recorded. In such systems we operate with the time average. In ergodic systems the time average mean squared displacement (TA MSD) $\overline{\delta^2}$, defined below, is the same as the ensemble average (EA MSD) $\langle x^2(t) \rangle = 2Dt$. So there is a unique way of defining the transport coefficient D in the sense that the two procedures are equivalent.

It is known that in complex and disordered systems the TA MSD might depend on the total measurement time t as well as on the lag time Δ [2]. Here we want to focus on non-stationary processes, with scale invariant correlation functions. There are many examples for such non-stationary scale invariant processes including the velocity of laser-cooled atoms [3], the motion of a tracer particle in a crowded environment [4], elastic models of fluctuating interfaces [5], diffusion in heterogeneous environment [6] and blinking quantum dots [7].

Since for scale invariant non stationary velocity correlation functions the EA MSD $\langle x^2(t) \rangle = 2D_\nu t^\nu$ is not equivalent to the TA MSD, we need two scaling Green-Kubo relations. The one for the EA MSD was investigated previously [8]. Here we focus on the time averaged

MSD of certain anomalous processes. We should remark, that the focus of the work of Dechant et al. [8] was on super diffusive processes while the approach in fact also works for subdiffusive processes when certain conditions on the exponents are met (see details below). A scaling Green-Kubo relation for time averages is obtained in chapter 3. Unlike for the EA MSD that was calculated in [8], it is now for the TA MSD important to know the scaling of the EA $\langle v^2(t) \rangle$ of the underlying velocity. We assume no net drift and $\langle x(t) \rangle = \langle v(t) \rangle = 0$.

This text is also a story about different models - stochastic and deterministic - that describe these processes. We will see differences in the results for such models which on the first sight look very similar. The calculation of the EA MSD and TA MSD for all kinds of cases and models has been of interest for scientists for a long time [2, 9–15]. In chapter 4 we apply the scaling Green-Kubo relation to a velocity renewal process and explicitly calculate the TA MSD. This was previously calculated by Tony Albers [11] for a similar model using a different technique.

In chapter 5 we compare our results to a jump model which is a random walk description of anomalous transport. It exhibits the same behavior in the EA MSD as the renewal velocity process. However, the TA MSD in the two models are very different. This implies that the TA MSD is an observable sensitive to underlying paths, if compared with the EA MSD.

In the end of this text we also want to introduce a third process which is completely deterministic. The idea of generating noise by deterministic chaotic processes goes back to [16]. One of the most prominent generators of anomalous dynamics in deterministic systems is the Pomeau-Manneville map (PM) [17]. It shows intermittent behavior i.e. alternating between chaotic bursts and long waiting times with much slower dynamics. It

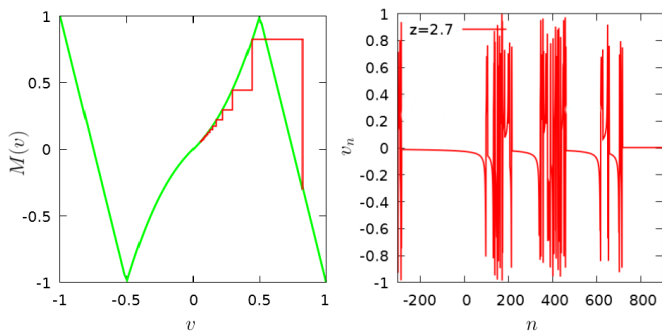


FIG. 1. The symmetrized Pomeau-Manneville map for $z = 2.3$. A velocity trajectory is shown in the right panel.

was connected to aging [18], weak ergodicity breaking [19] and anomalous diffusion [20]. We will be looking at pseudo-Brownian motion which is generated by a modified version of the map. The coordinate at discrete time t is given by $x_t = \sum_{i=0}^t v_i$. Here v_i is generated deterministically with PM type of map

$$v_{n+1} = M(v_n)$$

$$M(v) = \begin{cases} -4v - 3 & \text{for } v < -1/2 \\ v(1 + |2v|^{z-1}) & \text{for } |v| < 1/2 \\ -4v + 3 & \text{for } 1/2 < v \end{cases} . \quad (2)$$

Fig. 1 shows the map and a typical trajectory. The velocity in this model is bounded and $-1 < v < 1$. Two back to back unstable fixed points in the vicinity of $v = 0$ imply long power law distributed sticking times, with small velocity, interrupted by bursts and then an injection back to the vicinity of the indifferent fix point, i.e. this is the well known phenomenon of intermittency. We want to compare this deterministic process to two different stochastic models which will be introduced in chapter IV and V.

II. SCALE INVARIANT GREEN-KUBO RELATION

We consider diffusive processes with zero mean which in the long time limit

$$\langle x^2(t) \rangle = 2D_\nu t^\nu \quad (3)$$

and $\nu > 0$. The coordinate of the particle is given by $x(t) = \int_0^t v(t') dt'$ so initially $x(t)|_{t=0} = 0$. The random velocity process $v(t)$ has zero mean. The time averaged velocity correlation function determined empirically from the velocity path recorded in the time interval $(0, t)$ is

$$C_{\text{TA}}(t, \tau) = \frac{1}{t - \tau} \int_0^{t-\tau} dt_1 v(t_1) v(t_1 + \tau). \quad (4)$$

In general this correlation function, which is a functional of the random process $v(t)$ is random, namely specific

to the underlying velocity path. We assume that upon averaging the time averaged correlation function exhibits scale invariance namely

$$\langle C_{\text{TA}}(t, \tau) \rangle = C_{\text{TA}} t^{\nu-2} \phi_{\text{TA}} \left(\frac{\tau}{t} \right). \quad (5)$$

The averaging is with respect to an ensemble of paths $v(t)$ which can contain an average over initial conditions and stochastic histories, in experiment this correlation function is obtained from an ensemble of measured trajectories collected under some specified physical conditions. In physical systems such scale invariance is found in the scaling limit where both τ and t are large. However for now we assume the scale invariance works for all times which is an idealization. We now find the relation between the transport coefficient D_ν and the scale invariant time averaged correlation function.

First note that unlike stationary processes the time averaged correlation function is not identical to the ensemble average correlation function even in the long time limit. The ensemble average correlation function $C_{\text{EA}}(t + \tau, t) = \langle v(t)v(t + \tau) \rangle$ also exhibits scale invariance

$$C_{\text{EA}}(t + \tau, t) = C_{\text{EA}} t^{\nu-2} \phi_{\text{EA}} \left(\frac{\tau}{t} \right). \quad (6)$$

The correlation functions are related to one another according to [21]

$$C_{\text{TA}} \phi_{\text{TA}}(q) = \frac{q^{\nu-1}}{1-q} \int_{q/(1-q)}^{\infty} dy \frac{C_{\text{EA}} \phi_{\text{EA}}(y)}{y^\nu}. \quad (7)$$

This relation can be easily derived from the definition of the time averaged correlation function Eq. (4).

Since we have two related correlation functions, both of them can be used to find the transport coefficient D_ν . The relation between D_ν and the ensemble averaged correlation function was presented previously [8].

The MSD is

$$\langle x^2(t) \rangle = 2 \left\langle \int_0^t dt_1 v(t_1) \int_{t_1}^t dt_2 v(t_2) \right\rangle. \quad (8)$$

Switching variables of integration $t_1 = t_1$ and $t_2 = t_1 + \tau'$ we get

$$\langle x^2(t) \rangle = 2 \int_0^t d\tau' (t - \tau') \frac{\int_0^{t-\tau'} dt_1 \langle v(t_1) v(t_1 + \tau') \rangle}{t - \tau'}. \quad (9)$$

Using the definition of the time averaged correlation function and $q = \tau'/t$ we find

$$D_\nu = C_{\text{TA}} \int_0^1 dq (1-q) \phi_{\text{TA}}(q). \quad (10)$$

Using Eq. (7) and integration by parts we retrieve [8]

$$D_\nu = \frac{C_{\text{EA}}}{\nu} \int_0^\infty dq (1+q)^{-\nu} \phi_{\text{EA}}(q). \quad (11)$$

This is called a scaling Green-Kubo relation, since it connects between the aging correlation function and D_ν . While Eqs. (10,11) are clearly identical the appearance of two types of correlation functions implies that these tools should be used with some care. Theoreticians usually focus on the ensemble average correlation function, and then Eq. (11) is useful, but from data one may in principle obtain the time average scaling function $\phi_{\text{TA}}(q)$ and then Eq. (10) is worthy.

In our derivation we assumed that the integrals in Eqs. (10,11) are finite. This implies some limitations on the shape properties of correlation functions, which will soon be specified. We also assume that $\phi_{\text{EA}}(q)$ is positive valued, and all examples will focus on monotonically decaying functions. More explicitly we are limited by [8]

$$\begin{aligned} \phi_{\text{EA}}(q) &< c_1 q^{-\delta_1} \quad \text{with } 2 - \nu \leq \delta_1 < 1 \quad q \rightarrow 0 \\ \phi_{\text{EA}}(q) &< c_u q^{-\delta_u} \quad \text{with } \delta_u > 1 - \nu \quad q \rightarrow \infty. \end{aligned} \quad (12)$$

where $c_1 > 0$ and $c_u > 0$ are some constants. It is emphasized that these conditions are inequalities, namely we do not demand power law behaviors in the limits of $q \rightarrow 0$ and $q \rightarrow \infty$.

Here we used the exponents characterizing the ensemble average correlation function. One can use in principle exponents characterizing the time averaged correlation function instead. These exponents are related to one another, for example if the ensemble averaged correlation function behaves like $\phi_{\text{EA}}(q) \sim q^{-\delta_1}$ for $q \rightarrow 0$ so does the time averaged scaling function. This can be easily verified using Eq. (7). Similarly the coefficients \mathcal{C}_{TA} is proportional to \mathcal{C}_{EA} . From now on we will use the ensemble average correlation function $\phi_{\text{EA}}(q)$.

In the processes we consider below the variance of velocity is asymptotically

$$\langle v^2(t) \rangle \sim a \mathcal{C}_{\text{EA}} t^\beta \quad (13)$$

and

$$-1 \leq \beta < \nu - 1. \quad (14)$$

Note that in [8] the case $\beta > 0$ was considered, however the conditions for the theory to hold are not as limiting, and in fact the case $-1 < \beta < 0$ will be important in our example. The case $\beta = 0$ is of course natural in systems where the average kinetic energy of the particle is a constant. Now continuity demands

$$\phi_{\text{EA}}(q) \sim c_1 q^{-\delta_1} \quad (15)$$

for small q with

$$\delta_1 = 2 - \nu + \beta. \quad (16)$$

This is a useful relation since it gives the small q behavior of the correlation function in terms of exponents β and ν which are both measurable. In what follows we use the exponents β and ν to find the properties of the time averaged diffusion constant.

III. TIME AVERAGED MEAN SQUARED DISPLACEMENT

The time averaged MSD is

$$\overline{\delta^2} \equiv \frac{1}{t - \Delta} \int_0^{t-\Delta} [x(t_0 + \Delta) - x(t_0)]^2 dt_0. \quad (17)$$

Here t is the measurement time, namely the stochastic path $x(t')$ is recorded in the time interval $(0, t)$ and $\Delta \ll t$ is the lag time. For Brownian motion $\overline{\delta^2} \sim 2D\Delta$ so the time average procedure yields the diffusion constant recorded in ensemble measurement $\langle x^2(t) \rangle = 2Dt$. For scale invariant processes under consideration in this manuscript the identity of time and ensemble averages is broken. Further, the time average may remain a random variable even in the long time limit [2, 14, 15]. We will not address the fluctuations of this widely observed quantifier of diffusion processes, instead we focus on the ensemble average $\langle \overline{\delta^2} \rangle$.

Using Eq. (17) and $t \gg \Delta$ we get

$$\begin{aligned} \langle \overline{\delta^2} \rangle &\simeq \\ &\frac{1}{t} \int_0^{K\Delta} \langle [x(t_0 + \Delta) - x(t_0)]^2 \rangle dt_0 + \\ &\frac{1}{t} \int_{K\Delta}^t \langle [x(t_0 + \Delta) - x(t_0)]^2 \rangle dt_0. \end{aligned} \quad (18)$$

Here K is some large number satisfying $\Delta \ll K\Delta \ll t$. It is clear that in the limit of $t \rightarrow \infty$ only the second integral contributes and the first is negligible. Further in the second integral we have to find the MSD recorded between time t_0 and $t_0 + \Delta$ under the condition that $t_0 \gg \Delta$. We denote

$$\begin{aligned} \langle \Delta x^2(\Delta) \rangle_{t_0} &\equiv \langle [x(t_0 + \Delta) - x(t_0)]^2 \rangle = \\ 2\mathcal{C}_{\text{EA}} \int_0^\Delta dt_2 \int_0^{t_2} dt_1 (t_1 + t_0)^{\nu-2} \phi_{\text{EA}} \left(\frac{t_2 - t_1}{t_1 + t_0} \right). \end{aligned} \quad (19)$$

Since $\Delta \ll t_0$ it is clear that only the small q behavior of the correlation function is contributing to the integral in this limit, hence using Eqs. (15,16) one finds [8]

$$\langle \Delta x^2(\Delta) \rangle_{t_0} \sim 2 \frac{c_1 \mathcal{C}_{\text{EA}}}{(\nu - \beta - 1)(\nu - \beta)} (t_0)^\beta \Delta^{\nu-\beta}. \quad (20)$$

We can now derive our main equation in this section inserting Eq. (20) in Eq. (18) and performing a simple integral

$$\langle \overline{\delta^2} \rangle \sim \frac{2c_1 \mathcal{C}_{\text{EA}}}{(\beta + 1)(\nu - \beta - 1)(\nu - \beta)} t^\beta \Delta^{\nu-\beta}. \quad (21)$$

To determine the exponents of the time average mean square displacement indirectly, for example via a measurement, one needs to know β which is a measure of the increase or decrease of kinetic energy of the particle, and ν which as mentioned can be determined from ensemble averaged measurements of the MSD. Of course one can turn this around: with the time average exponents and β one can get ν and hence the ensemble averaged exponent. Here we see that the time averaged MSD is very

different from the ensemble average. It depends on the total measurement time t and the lag time Δ . When $\beta = 0$ meaning that $\langle v^2 \rangle$ is a constant, as one finds in normal thermal systems, and when $\nu = 1$ as found for normal transport, the time average behaves normally as expected $\langle \delta^2 \rangle \propto \Delta$. This case corresponds to the standard Green-Kubo relation and Eq. (21) does not hold. If kinetic energy is not increasing, i.e. $\beta = 0$, the time averaged MSD $\overline{\delta^2} \propto \Delta^\nu$ so it exhibits the same time dependence as does the ensemble average. Notice that unlike the ensemble average MSD, where D_ν depends on the details of the correlation function namely on $\phi_{\text{EA}}(q)$ in the range $0 < q < \infty$ the time averaged MSD is determined by $c_1 \mathcal{C}_{\text{EA}}$ namely by the behavior of this function close to $q \rightarrow 0$.

IV. RENEWAL VELOCITY PROCESS

We consider a renewal process $v(t)$ which will be used to demonstrate the general theory derived so far. At random times t_0, t_1, t_2, \dots the particle experiences ‘strong collisions’ in such a way that the velocity $v(t)$ is totally randomized, i.e., the correlation between the velocities of the particle before and after a collision event is zero.

Between the collision events particles move deterministically. Let n be the random number of collision events in the time interval $(0, t)$ and the process starts at the origin of time namely $t_0 = 0$. Here time $t_n < t$ is the time when last stochastic modification of velocity took place. At time t the velocity is

$$v(t) = v_{\gamma, n} \gamma (t - t_n)^{\gamma-1} \quad (22)$$

and we consider the case $0 < \gamma$ (the case $\gamma < 0$ is of interest, at least mathematically and it can yield subdiffusion). The case $\gamma = 1$ implies motion at constant velocity between collision events. Here $v_{\gamma, n}$ is a random variable with zero mean and finite variance. The process starts at time $t = 0$ and the waiting times between the renewal events are independent identically distributed random variables with a common probability density function (PDF) $\psi(\tilde{\tau})$ and $\tilde{\tau} > 0$. Similarly the coefficients $v_{\gamma, j}$ are mutually independently distributed random variables taken of a distribution $f(v_\gamma)$, with zero mean and finite variance denoted $\langle (v_\gamma)^2 \rangle$. So to describe the process we generate the pair $(\tilde{\tau}_0, v_{\gamma, 0})$ say on a computer, and then for times shorter than $t_1 = \tilde{\tau}_0$ the velocity is $v(t) = v_{\gamma, 0} \gamma t^{\gamma-1}$. Then the process is renewed, namely the pair $(\tilde{\tau}_1, v_{\gamma, 1})$ is used and in the time interval $t_1 < t < t_2 = \tilde{\tau}_0 + \tilde{\tau}_1$ the velocity is $v(t) = v_{\gamma, 1} \gamma (t - t_1)^{\gamma-1}$, etc. A trajectory of the process is presented in Fig. 2.

A. Velocity correlation function

We now investigate the velocity correlation function. We will focus on widely used fat tailed waiting time PDFs

$$\psi(\tilde{\tau}) \sim A \tilde{\tau}^{-(1+\alpha)} \quad \text{when } \tilde{\tau} \rightarrow \infty \quad (23)$$

and $\alpha > 0$ for normalizability. We note that even exponential statistics gives certain strong anomalies when $\gamma < 0$, a case we do not study here. The mean waiting time is infinite if $0 < \alpha < 1$ while the second moment of the same variable diverges when $0 < \alpha < 2$ (we will not consider marginal cases like $\alpha = 1$ as they bring with them logarithmic corrections).

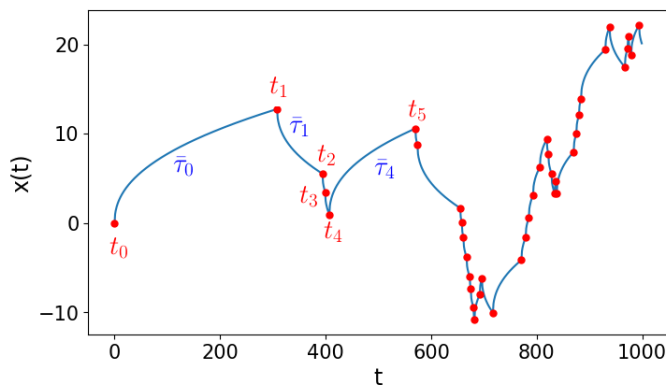


FIG. 2. A schematic diagram of a trajectory $x(t)$ for a renewal velocity process with $v_{\gamma, n} = \pm 1$ with equal probability. The parameters are $\alpha = 5/14$, $\gamma = 2/7$. The renewals occur at the times t_0, t_1, \dots marked with red dots. The waiting times in between are denoted with $\tilde{\tau}_0, \tilde{\tau}_1, \dots$ and t denotes the total measurement time.

We use methods similar to those used by Godreche and Luck [22]. Let $C_n(t, \tau) \equiv \langle v(t)v(t+\tau) \rangle_n$ be the velocity correlation function for a process with n collisions in the time interval $(0, t)$. We will obtain this function and summation over n will yield the sought after correlation function $\langle v(t)v(t+\tau) \rangle = C(t, \tau) = \sum_{n=0}^{\infty} C_n(t, \tau)$.

We define the double Laplace transform

$$C_n(s, u) = \int_0^{\infty} e^{-st} dt \int_0^{\infty} e^{-u\tau} d\tau \langle v(t)v(t+\tau) \rangle_n. \quad (24)$$

The velocity is correlated only if $t_n < t < t + \tau < t_{n+1}$ namely when the observation times fall within the same epoch of travel. This is clearly the case since the velocities $v_{\gamma, j}$ are not correlated. We therefore have using Eq. (22)

$$\hat{C}_n(s, u) = \langle v_{\gamma}^2 \rangle \gamma^2 \langle \int_0^{\infty} e^{-st} dt \int_0^{\infty} e^{-u\tau} d\tau (t - t_n)^{\gamma-1} (t + \tau - t_n)^{\gamma-1} \theta(t_n < t < t_{n+1}) \theta(t_n < t_n + \tau < t_{n+1}) \rangle. \quad (25)$$

Here $\theta(\dots) = 1$ if the condition in the parenthesis is valid otherwise the theta function is zero, so $\theta(\dots)$ is a square pulse function. The average is with respect to the time process. Switching integration variables according to $t - t_n = y$ and using $t_{n+1} - t_n = \tilde{\tau}_n$ we find

$$\hat{C}_n(s, u) = \gamma^2 \langle (v_{\gamma})^2 \rangle \langle e^{-t_n s} \int_0^{\tilde{\tau}_n} dy e^{-sy} y^{\gamma-1} \int_0^{\tilde{\tau}_n - y} d\tau e^{-u\tau} (y + \tau)^{\gamma-1} \rangle. \quad (26)$$

From renewal assumption the random variables t_n and τ_{n+1} are independent. Further since $t_n = \sum_{j=0}^{n-1} \tilde{\tau}_j$ and because the waiting times are also independent we have $\langle \exp(-st_n) \rangle = \hat{\psi}^n(s)$ where $\hat{\psi}(s)$ is the Laplace $\tilde{\tau} \rightarrow s$ transform of $\psi(\tilde{\tau})$. The remaining average is with respect to $\tilde{\tau}_n$ which is a random variable drawn from $\psi(\tilde{\tau})$. Hence we get

$$\hat{C}_n(s, u) = \gamma^2 \langle (v_{\gamma})^2 \rangle \hat{\psi}^n(s) \int_0^{\infty} d\tilde{\tau} \psi(\tilde{\tau}) \int_0^{\tilde{\tau}} dy e^{-sy} y^{\gamma-1} \int_0^{\tilde{\tau}-y} d\tau e^{-u\tau} (y + \tau)^{\gamma-1}. \quad (27)$$

Let us denote

$$W(\tilde{\tau}) = \int_{\tilde{\tau}}^{\infty} d\tilde{\tau}' \psi(\tilde{\tau}'), \quad (28)$$

which is the probability of not experiencing a renewal/collision in the time interval $(0, \tilde{\tau})$. Then clearly

$$\hat{C}_n(s, u) = \gamma^2 \langle (v_{\gamma})^2 \rangle \hat{\psi}^n(s) \int_0^{\infty} d\tilde{\tau} \left[-\frac{d}{d\tilde{\tau}} W(\tilde{\tau}) \right] \int_0^{\tilde{\tau}} dy e^{-sy} y^{\gamma-1} \int_0^{\tilde{\tau}-y} d\tau e^{-u\tau} (y + \tau)^{\gamma-1}. \quad (29)$$

We now integrate by parts, and then the geometric series $\sum_{n=0}^{\infty} \hat{\psi}^n(s) = 1/[1 - \hat{\psi}(s)]$ gives

$$\hat{C}(s, u) = \frac{\gamma^2 \langle (v_{\gamma})^2 \rangle}{1 - \hat{\psi}(s)} \int_0^{\infty} d\tilde{\tau} W(\tilde{\tau}) \tilde{\tau}^{\gamma-1} e^{-u\tilde{\tau}} \int_0^{\tilde{\tau}} dy e^{-(s-u)y} y^{\gamma-1}. \quad (30)$$

In principle the double inverse Laplace transform of this expression yields the velocity correlation function $\langle v(t)v(t+\tau) \rangle \equiv C(t, \tau)$. We can invert from u to τ rather easily, since the inverse Laplace transform of $\exp(-ux)$ is a delta function $\delta(\tau - x)$, hence we find

$$C(s, \tau) = \frac{\gamma^2 \langle (v_{\gamma})^2 \rangle}{1 - \hat{\psi}(s)} \int_{\tau}^{\infty} d\tilde{\tau} W(\tilde{\tau}) \tilde{\tau}^{\gamma-1} (\tilde{\tau} - \tau)^{\gamma-1} e^{-s(\tilde{\tau}-\tau)}. \quad (31)$$

When $\gamma = 1$ Eq. (30) gives

$$\hat{C}(s, u) = \frac{\langle (v_1)^2 \rangle}{1 - \hat{\psi}(s)} \frac{\hat{W}(s) - \hat{W}(u)}{u - s}, \quad (32)$$

where $\hat{W}(s)$ is the Laplace transform of $W(\tilde{\tau})$ and from the convolution theorem $\hat{W}(s) = [1 - \hat{\psi}(s)]/s$.

B. Long time limit with finite mean sojourn time

We now classify behaviors of the correlation function in the limit of long time t . We first consider the case when the average waiting time $\langle \tilde{\tau} \rangle = \int_0^\infty d\tilde{\tau} \tilde{\tau} \psi(\tilde{\tau})$ is finite hence $\alpha > 1$. In this case the small s behavior of $\hat{\psi}(s)$ is

$$\hat{\psi}(s) \sim 1 - \langle \tilde{\tau} \rangle s \quad (33)$$

and similarly for the small u behavior of $\hat{\psi}(u)$. The small s behavior gives the large t limit of the correlation function, so using the small s expansion $\exp[-s(\tilde{\tau} - \tau)]/[1 - \hat{\psi}(s)] \sim 1/(s\langle \tilde{\tau} \rangle)$ and inverting, i.e. the inverse Laplace transform of $1/s$ is 1, we find using Eq. (31)

$$\lim_{t \rightarrow \infty} C(t, \tau) = \frac{\gamma^2 \langle (v_\gamma)^2 \rangle}{\langle \tilde{\tau} \rangle} \int_\tau^\infty d\tilde{\tau} W(\tilde{\tau}) \tilde{\tau}^{\gamma-1} (\tilde{\tau} - \tau)^{\gamma-1}. \quad (34)$$

When $\gamma = 1$

$$\lim_{t \rightarrow \infty} C(t, \tau) = \frac{\langle (v_1)^2 \rangle}{\langle \tilde{\tau} \rangle} \int_\tau^\infty d\tilde{\tau} W(\tilde{\tau}), \quad (35)$$

which is known to the experts.

If the waiting time PDF is exponential with unit mean $\psi(\tilde{\tau}) = \exp(-\tilde{\tau})$ for $\tilde{\tau} > 0$ we have $\langle \tilde{\tau} \rangle = 1$ and

$$\lim_{t \rightarrow \infty} C(t, \tau) = \gamma^2 \langle (v_\gamma)^2 \rangle \int_\tau^\infty d\tilde{\tau} e^{-\tilde{\tau}} \tilde{\tau}^{\gamma-1} (\tilde{\tau} - \tau)^{\gamma-1}. \quad (36)$$

So when $\gamma < 0$ the integral diverges, an indication to non-normal behavior not investigated in this paper. For the case $\gamma = 1/2$ and $\langle (\gamma v_\gamma)^2 \rangle = 1$ we get

$$\lim_{t \rightarrow \infty} C(t, \tau) = e^{-\tau/2} K_0(\tau/2). \quad (37)$$

This blows up at $\tau \rightarrow 0$ and in that limit $\lim_{t \rightarrow \infty} C(t, \tau) \sim -\log(\tau)$. So even for exponential waiting times we get non trivial behaviors when $\gamma \leq 1/2$ an effect which is related to the fact that for $\gamma < 1$ the velocity blows up immediately after a renewal. The divergence of the correlation function at $\tau = 0$ means that the second moment of $v(t)$ defined in Eq. (22) is diverging, in reality this implies that the variance is increasing with time t and for any finite long time we expect a finite variance.

Returning to fat tailed sojourn time PDF Eq. (23) we have in the limit of long waiting times

$$W(\tilde{\tau}) \sim \frac{A \tilde{\tau}^{-\alpha}}{\alpha}. \quad (38)$$

Hence in the limit of long τ we get from Eq. (34) and $\alpha > 1$

$$\lim_{t \rightarrow \infty} C(t, \tau) \sim \frac{\langle (\gamma v_\gamma)^2 \rangle}{\langle \tilde{\tau} \rangle} \frac{c_3 A}{\alpha} \tau^{2\gamma-1-\alpha}. \quad (39)$$

Here $2\gamma < 1 + \alpha$ and $c_3 = \int_1^\infty dx x^{\gamma-1-\alpha} (x-1)^{\gamma-1}$. Eq. (39) is an example of a scale invariant correlation function, which is of the non aging type.

So far we have considered the limit $t \rightarrow \infty$. As we have just shown, this led to meaningless results in some cases, as the integrals diverge, e.g. $c_3 = \infty$ for $2\gamma > 1 + \alpha$. So we consider the case when t and also τ are long but finite. Returning back to Eq. (31) we use the approximation, valid for large t or small s ,

$$\frac{\exp[-s(\tilde{\tau} - \tau)]}{1 - \hat{\psi}(s)} \sim \frac{\exp[-s(\tilde{\tau} - \tau)]}{s\langle \tilde{\tau} \rangle}. \quad (40)$$

Using convolution theorem of Laplace transform the inverse Laplace transform ($s \rightarrow t$) of the expression on the RHS is a pulse function equal 1 if $0 < \tilde{\tau} - \tau < t$ otherwise it is zero. Hence inverting Eq. (31) in the limit of long t

$$C(t, \tau) \simeq \frac{\langle (\gamma v_\gamma)^2 \rangle}{\langle \tilde{\tau} \rangle} \int_\tau^{t+\tau} d\tilde{\tau} W(\tilde{\tau}) \tilde{\tau}^{\gamma-1} (\tilde{\tau} - \tau)^{\gamma-1}. \quad (41)$$

When τ is large in such a way that $W(\tilde{\tau})$ for $\tilde{\tau} > \tau$, is described by Eq. (38) we find

$$C(t, \tau) \simeq \frac{\langle (\gamma v_\gamma)^2 \rangle A}{\langle \tilde{\tau} \rangle \alpha} \tau^{2\gamma-1-\alpha} \int_1^{1+t/\tau} dx x^{\gamma-1-\alpha} (x-1)^{\gamma-1}. \quad (42)$$

This in the limit $t/\tau \rightarrow \infty$ recovers Eq. (39) when $2\gamma < 1 + \alpha$. If $t/\tau \gg 1$ and the conditions $2\gamma > \alpha + 1$, $\gamma > 0$, $\alpha > 1$ hold $C(\tau, t) \propto t^{2\gamma-1-\alpha}$.

Clearly Eq. (42) belongs to the class of scaling correlation functions described by Eq. (6). We can now summarize and find the exponents and pre-factors describing both the ensemble and time averaged transport. We have

$$\mathcal{C}_{\text{EA}} = \frac{\langle (\gamma v_\gamma)^2 \rangle A}{\alpha \langle \tilde{\tau} \rangle} \quad (43)$$

the ensemble averaged transport exponent is

$$\nu = 2\gamma + 1 - \alpha > 1. \quad (44)$$

The ensemble averaged scaling correlation function

$$\phi_{\text{EA}}(q) = q^{2\gamma-1-\alpha} \int_1^{1+1/q} dx x^{\gamma-1-\alpha} (x-1)^{\gamma-1}. \quad (45)$$

In the small q limit we have $\phi_{\text{EA}}(q) \sim c_1 q^{-\delta_1}$ as in Eq. (15) and the exponent β is obtained from Eq. (16). We find

$$\begin{aligned} \delta_1 = -2\gamma + 1 + \alpha, & \quad \beta = 0, & \quad c_1 = c_3, & \quad \text{if } \alpha < 2\gamma < 1 + \alpha \\ \delta_1 = 0, & \quad \beta = \nu - 2 = 2\gamma - \alpha - 1, & \quad c_1 = (2\gamma - \alpha - 1)^{-1}, & \quad \text{if } 1 + \alpha < 2\gamma. \end{aligned} \quad (46)$$

The condition $\delta_u > 1 - \nu$ also holds. Note that the transition between the two behaviors is found for $2\gamma = 1 + \alpha$ and then $\nu = 2$, so a qualitative transition takes place when the ensemble averaged mean square displacement is ballistic. With the information in Eq. (46) we may apply the scaling Green-Kubo relation and predict the time averaged MSD.

C. Long time limit with diverging mean sojourn time

We now consider the case $0 < \alpha < 1$ so here the mean flight time is infinite. The small s expansion of the Laplace transform of the PDF of waiting times is

$$\hat{\psi}(s) \sim 1 - \frac{A\Gamma(1-\alpha)}{\alpha} s^\alpha + \dots \quad (47)$$

where $\Gamma(\cdot)$ is the Gamma function. In the limit of large τ we insert Eqs. (38,47) in Eq. (31)

$$C(s, \tau) \simeq \frac{\langle (\gamma v_\gamma)^2 \rangle}{\Gamma(1-\alpha)} \int_\tau^\infty d\tilde{\tau} \tilde{\tau}^{\gamma-1-\alpha} \frac{e^{-s(\tilde{\tau}-\tau)}}{s^\alpha} (\tilde{\tau}-\tau)^{\gamma-1}, \quad (48)$$

an asymptotic equation that does not depend on the amplitude A or any other detail on $\psi(\tilde{\tau})$ besides the exponent α . To invert this formula from s to t we use the convolution theorem of Laplace transform, the Laplace pairs $1/s^\alpha \leftrightarrow t^{\alpha-1}/\Gamma(\alpha)$, $\exp[-s(\tilde{\tau}-\tau)] \leftrightarrow \delta[t - (\tilde{\tau}-\tau)]$ to find

$$\frac{e^{-s(\tilde{\tau}-\tau)}}{s^\alpha} \leftrightarrow \begin{cases} 0 & \tilde{\tau} - \tau < 0 \\ \frac{1}{\Gamma(\alpha)[t - (\tilde{\tau}-\tau)]^{1-\alpha}} & \text{otherwise} \\ 0 & t < \tilde{\tau} - \tau. \end{cases} \quad (49)$$

This is used to invert Eq. (48)

$$C(t, \tau) \simeq \frac{\langle (\gamma v_\gamma)^2 \rangle}{\Gamma(1-\alpha)\Gamma(\alpha)} t^{2\gamma-2} \phi_{\text{EA}}(q) \quad (50)$$

with

$$\phi_{\text{EA}}(q) = \int_q^{1+q} dx x^{\gamma-1-\alpha} [1 - (x-q)]^{\alpha-1} (x-q)^{\gamma-1} \quad (51)$$

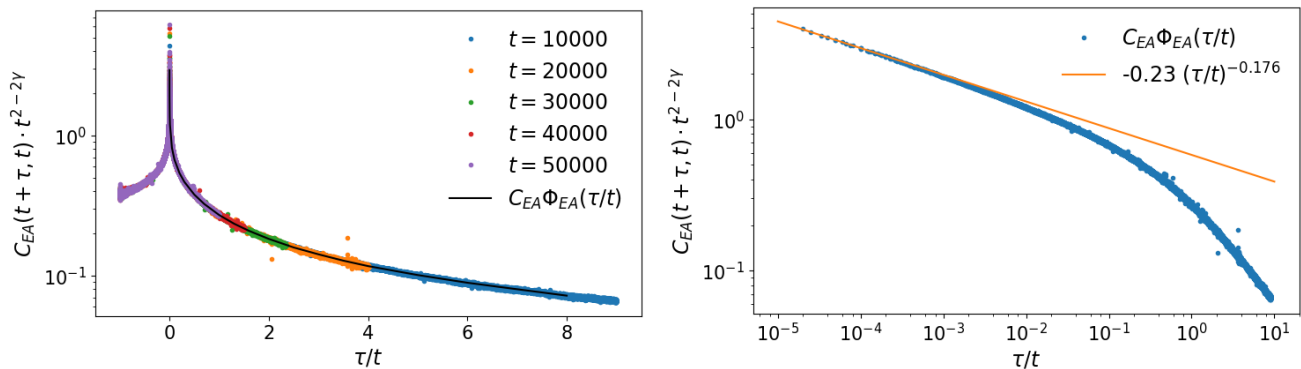


FIG. 3. Scaled correlation function of a renewal velocity process with $v_{\gamma,n} = \pm 1$ for $\alpha = 5/13$, $\gamma = 8/13$. The abscissa shows the fraction $q = \tau/t$ while the ordinate is rescaled by $t^{2-\nu}$. Thus the graph shows the function Φ_{EA} (Eq. (51)), multiplied by C_{EA} . Simulations for different times nicely match to theory. Left: the theory curve is drawn in black. It is universal for different t . Right: log-log plot shows behavior for $\tau/t \rightarrow 0$. The fitted scaling exponent corresponds to the parameter δ_1 and is therefore directly related to β . It matches reasonably well with the theory from Eq. (53) which predicts $\delta_1 = 0.154$.

and $q = \tau/t$. It is now easy to read off this equation the expressions relevant for the calculation of the time averaged mean square displacement. In particular using Eq. (6) the anomalous diffusion scaling exponent is

$$1 < \nu = 2\gamma \quad (52)$$

and clearly $C_{EA} = \langle (\gamma v_\gamma)^2 \rangle / [\Gamma(1-\alpha)\Gamma(\alpha)] = \langle (\gamma v_\gamma)^2 \rangle \sin(\pi\alpha) / \pi$. We then find

$$\begin{aligned} \delta_1 = 0, & \quad \beta = \nu - 2 = 2\gamma - 2, & c_1 = \int_1^\infty dy y^{-2\gamma+1} (y-1)^{\alpha-1}, & \text{if } 2\gamma > 1 + \alpha \\ \delta_1 = \alpha + 1 - 2\gamma, & \beta = \alpha - 1, & c_1 = [1 + \alpha - 2\gamma]^{-1}, & \text{if } 2\gamma < 1 + \alpha. \end{aligned} \quad (53)$$

A plot of the scaled correlation function is shown in Fig. 3. Again with this information the scaling Green-Kubo formalism predicts the behaviors of the time averaged MSD, of course under the conditions that the theorem holds, e.g. $-1 < \beta$ and $\nu - \beta > 1$. For large q , $\phi_{EN} \propto q^{-\delta_u}$ with $\delta_u = 1 + \alpha - \gamma$ so the condition $\delta_u > 1 - \nu$ in Eq. (12) holds.

For ballistic Levy walks we have $\gamma = 1$ and then the condition $2\gamma > 1 + \alpha$ holds (since here $\alpha < 1$) and hence in that case we have only one type of behavior [the first line in Eq. (53)]. So for Levy walks $\nu = 2$, $\beta = 0$, $c_1 = \pi csc(\pi\alpha)$ and using a well known identity for Gamma functions $C_{EA} c_1 = \langle (v_1)^2 \rangle$. Hence we find using Eq. (21) $\langle \bar{\delta}^2 \rangle \sim \langle (v_1)^2 \rangle \Delta^2$. This was obtained in [13, 24] and there also the corrections to this formula were investigated, as well as the fluctuations of the time average $\bar{\delta}^2$.

D. Phase Diagram

Now with the information on the exponents β describing variance of velocity and ν describing the variance of position in ensemble averaged sense, we easily obtain the phase diagram of the time averaged mean square displacement using Eq. (21). We focus on $0 < \gamma < 2$ then in the case of diverging averaged waiting time $0 < \alpha < 1$ and using Eq. (52,53) we find

$$\langle \bar{\delta}^2 \rangle \propto \begin{cases} t^{\alpha-1} \Delta^{2\gamma-\alpha+1} & \max(0, 2\gamma - 1) < \alpha < \min(1, 2\gamma) \\ t^{2\gamma-2} \Delta^2 & 0 < \alpha < \min(1, 2\gamma - 1) \end{cases}. \quad (54)$$

This was obtained in [11], where a CTRW approach was used. We see that the motion is super-ballistic or ballistic and the time average may either increase (an effect called rejuvenation) or decrease (called aging) with total measurement time. As mentioned it is controlled by the value of the exponent β , describing time dependence of the kinetic energy. For the case of finite average sojourn time $1 < \alpha < 2$ but diverging variance we use Eqs. (44,46) to find

$$\langle \bar{\delta}^2 \rangle \propto \begin{cases} t^0 \Delta^{2\gamma+1-\alpha} & \max(1, 2\gamma - 1) < \alpha < \min(2, 2\gamma) \\ t^{2\gamma-\alpha-1} \Delta^2 & 1 < \alpha < \min(2\gamma - 1, 2) \end{cases}. \quad (55)$$

V. RANDOM WALKS

The velocity process under investigation is related to the coupled continuous time random walk model [25–31].

We now investigate a closely related random walk, which

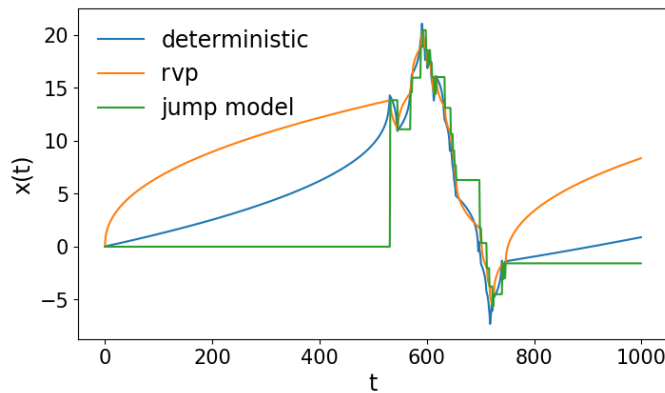


FIG. 4. Trajectories of all three processes: A deterministic process generated by the Pomeau-Manneville map, a renewal velocity process (rvp) with $v_{\gamma,n} = \pm 1$ and a random walk. The parameters are $z = 2.8$, $\alpha = 5/14$, $\gamma = 2/7$. At the renewal times both stochastic processes are identical and the deterministic model is also approximately the same. In between these points the trajectories behavior is very different. The deterministic trajectory lies in between the two others.

is not based on a velocity picture. Our goal is to show that the TA in both models are non-identical (unlike the ensemble averages). This implies that while random walk theory can work well in the ensemble average sense, when it comes to predictions of time averages it must be used with care.

A random walker waits localized in space and then makes a jump. The waiting times in this well known model are independently identically distributed random variables drawn from the PDF $\psi(\tau)$. The size of each independent spatial step is χ and we treat the case of equal probabilities of jumping to the left or right (no bias). In coupled processes the jump length and the waiting times are correlated and an example of their joint PDF is

$$\psi(\chi, \tau) = \psi(\tau) \frac{1}{2} [\delta(\chi - \tau^\gamma) + \delta(\chi + \tau^\gamma)]. \quad (56)$$

This seems at first glance very similar to our process when the velocities $v_{\gamma,n}$ are either $+1$ or -1 with equal probability. Indeed the random size χ_j of displacement j in the velocity model is $\chi_j = v_{\gamma,j}(\tilde{\tau}_j)^\gamma$ so displacements in both approaches are identical (the displacement in the velocity model is simply the length traveled between renewal events). However the two models differ in the path in between renewal events. In our case the velocity is always finite (unless $v_{\gamma,j}$ is zero). In the coupled CTRW particles wait and then jump, so the velocity is nearly always zero (see Fig. 4). Still position of the particle at time t_n is the same in both models. Hence the distribution of the position at this time is identical. Also the ensemble averaged MSD shows the same scaling as we see when comparing the results in [10] to Eq. (52)

$$\langle x^2 \rangle \approx \begin{cases} \frac{\Gamma(2\gamma-\alpha)}{|\Gamma(-\alpha)|\Gamma(1+2\gamma)} t^{2\gamma} & \text{if } 2\gamma > \alpha \\ \frac{\langle \tau^{2\gamma} \rangle}{c\Gamma(\alpha+1)} t^\alpha & \text{if } 2\gamma < \alpha \end{cases} \quad (57)$$

for $0 < \alpha < 1$.

However, as we show below the time averaged MSD in these models are very different. In particular the exponents describing the time averaged MSD in both models are not the same. We write the velocity of a jump model in the (not rigorous) form

$$v(t) = \sum_{\{i:t_i < t\}} \chi_i \delta(t - t_i) \quad (58)$$

and assume that its ensemble average of the square scales like $\langle v^2(t) \rangle \propto t^\beta$. We further assume that the scale invariant Green-Kubo relation holds for such processes. Then we see that the TA MSD of such a jump process always depends linearly on Δ . The EA MSD

$$\langle x^2(t) \rangle = \left\langle \int_0^t dt_1 v(t_1) \int_0^t dt_2 v(t_2) \right\rangle \quad (59)$$

can be rewritten with the θ -step function and the integral over $\delta(t)$

$$\langle x^2(t) \rangle = \left\langle \sum_{ij} \chi_i \chi_j \theta(t - t_i) \theta(t - t_j) \right\rangle. \quad (60)$$

Using $\langle \chi_i \chi_j \rangle = \delta_{ij}$, this yields

$$\langle x^2(t) \rangle = \left\langle \left(\int dt v(t) \right)^2 \right\rangle = \int dt \langle (v(t))^2 \rangle \propto t^{\beta+1} \quad (61)$$

and therefore $\beta = \nu - 1$. Using the ensemble averaged exponent ν given in Eq. (57) together with β we find using Eq. (21)

$$\langle \overline{\delta^2} \rangle \sim \begin{cases} t^{2\gamma-1} \Delta & \text{if } 2\gamma > \alpha \\ t^{\alpha-1} \Delta & \text{if } 2\gamma < \alpha \end{cases}. \quad (62)$$

These equations were derived previously in [10] from the underlying random walk. Here we have demonstrated that we can easily get β and once ν is known predict the behavior of the TA MSD.

The result differs from the velocity model (Eq. 54) not only in the pre-factors but also in the exponents. Thus the time average being sensitive to the whole shape of the path, needs a precise definition of the model. And in this sense simplified random walks which neglect the details of the velocity path can be widely different if compared to velocity models. The second difference between models is the propagation between last renewal event and measurement time t . In wait and then jump process the particle is stuck in this last interval, while in the velocity model it continues traveling. For long tailed PDF $\psi(\tilde{\tau})$ the statistics of this last traveling event is known to be of importance, for the calculation of quantities like D_ν , however this effect does not modify exponents describing the ensemble averaged mean square displacement.

VI. THE DETERMINISTIC SYSTEM

We will now look at the deterministic process defined in (2) and compare it to the two stochastic processes above. At time $t = 0$ the initial velocity is uniformly

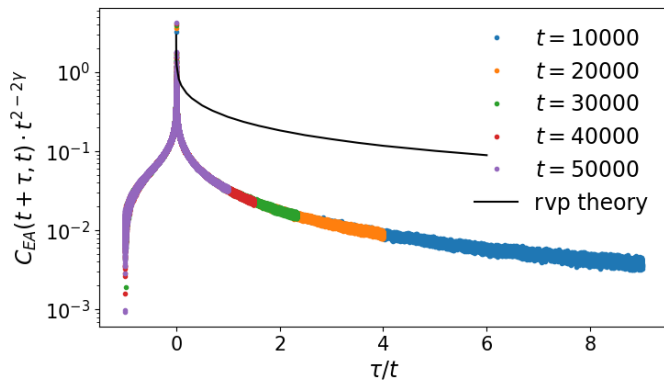


FIG. 5. Scaled correlation function of the deterministic process with $z = 3.6$ ($\alpha = 5/13$, $\gamma = 8/13$). The abscissa shows the fraction $z = \tau/t$ while the ordinate is rescaled by $t^{2-\nu}$. The black curve is proportional to the function Φ_{EA} of the renewal velocity process (rvp), that was already shown in Fig. 3. It strongly differs from the numerical result of the deterministic process.

distributed in the interval $[-1, 1]$. We generate on the computer the velocity path, just by iterating the map, and from this we obtain the coordinate x_t and hence the time average MSD. The symmetry of initial conditions and of the map itself insures that we do not have any drift. In Fig. 5 we see that the correlation function of the map is scale invariant. We have chosen z such that $\alpha = 0.59$ and $\gamma = 0.41$ (see next section) thus the scale invariant Green-Kubo relation holds.

A. The connection between the parameter z , the waiting times and the jump lengths

Let us first get an idea about waiting times and jump lengths in the process. Roughly speaking, in the long time limit, properties of the map in the vicinity of the unstable fixed point determine the statistical behavior of the paths. For $v > 0$ the map is approximated with a differential equation

$$\frac{dv}{dt} = \tilde{a}v^z \quad \text{when } v \rightarrow 0, \quad (63)$$

with $\tilde{a} > 0$ and for the specific example in Eq. (2) $\tilde{a} = 2$. Let $\alpha = 1/(z-1) > 0$, it is well known that the PDF of sojourn times in the vicinity of the indifferent points is given by [23]

$$\psi(\tilde{\tau}) \propto (\tilde{\tau})^{-1-\alpha}. \quad (64)$$

This is obtained from Eq. (63). It is easy to integrate Eq. (63),

$$\frac{\alpha}{\tilde{a}} \left[\frac{1}{(v_0)^{1/\alpha}} - \frac{1}{(v_t)^{1/\alpha}} \right] = t \quad (65)$$

and calculate the time it takes v_t starting on v_0 to hit v_b . Here v_b is some small constant on which roughly speaking the continuous approximation of the map breaks down, say $v_b = 1/4$. Importantly it is an irrelevant parameter in the sense that eventually our results do not depend on its specific value. Using uniform distribution of initial conditions v_0 , one obtains Eq. (64) which is well backed by simulations and theory.

We now need to find the exponent γ . First note that the displacement during a renewal interval of length $\tilde{\tau}$, which we denote χ is by definition statistically proportional to $\tilde{\tau}^\gamma$. For the map we need to find

$$\chi = \int_0^{\tilde{\tau}} v_t dt. \quad (66)$$

where v_0 is the injection point, marking the start of the escape from the unstable point, and $\tilde{\tau}$ is the time to reach the boundary (when reinjection is taking place again). Using the fact that initial velocity v_0 is much smaller than its boundary value $0 < v_0 \ll v_b$ we find the scaling relation between the velocity at the start of the renewal (the injection point) and the time until particle hits the boundary $v_0 \simeq [\alpha/(\tilde{a}\tilde{\tau})]^\alpha$. Of course not all the injection points v_0 are far from v_b , however those injection events which land in vicinity of v_b quickly escape and do not control the long time limit of the problem under investigation. Here we use $v_t > 0$, however in the dynamics generated by the map both positive and negative velocities are equally probable, and the sign of the velocity is determined merely by the injection point, namely does it happen to fall to the left or right of $v = 0$. Inserting Eq. (65) in Eq. (66) we find that in statistical sense

$$\chi \propto \frac{\alpha}{\tilde{a}(1-\alpha)} \left(\frac{\tilde{\tau}\tilde{a}}{\alpha} \right)^{1-\alpha}. \quad (67)$$

Hence to summarize we have that the non linear parameter of the map $z > 1$ gives

$$\alpha = \frac{1}{z-1}, \quad \gamma = \frac{z-2}{z-1}. \quad (68)$$

Using Eq. (52) we find

$$\nu = 2 \left(\frac{z-2}{z-1} \right) \quad (69)$$

for the parameter range where our theory is applicable. As we will see this is true for $z > 2.5$. In Fig. 5 the prediction Eq. (69) is tested as we plot $t^{2-\nu}C_{EA}(t + \tau, t)$ versus τ/t observing a data collapse. In Fig. 6 we see the scaling exponents of the EA MSD of all three processes compared to each other. They are all the same. For

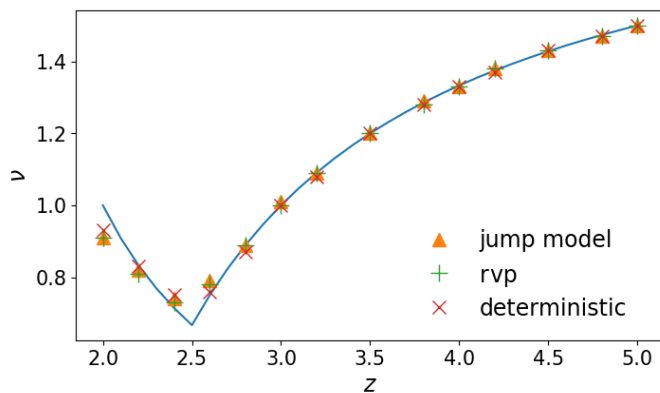


FIG. 6. The scaling exponent ν of the ensemble averaged mean squared displacement for all three processes. The solid line illustrates the theory (Eq. (69),[10]). The scaling exponent was fitted for times $10^4 < t < 10^6$. The averaging for all three models was done over 10000 trajectories.

$z < 2$ ($\alpha > 1$) the mean sojourn time is finite and therefore the processes exhibit normal diffusion. The range $2 < z < 2.5$ can also be understood. Here the statistics is completely dominated by the waiting times and the jump sizes/ velocities are small. It was investigated for example in [10] and is also related to the spatial diffusion of the Pomeau-Manneville map described in [23].

B. The exponent β and infinite ergodic theory

The standard setting of the classical Green-Kubo relation is for a system in contact with a heat bath and then the velocity distribution is Maxwellian. The processes under study are certainly non-thermal and as we now demonstrate the velocity fluctuations are described by infinite ergodic theory provided that $0 < \alpha = 1/(z-1) < 1$. Here we will use this theory to derive β in a direct way. Let $\rho(|v|, t)$ be the normalized density of the variable $|v|$ at time t . This density is in principle obtained with the PM transformation starting from a smooth density say a uniform density in $|v| < 1$ (by smooth we mean in particular that initially the density does not contain a delta function). For standard ergodic transformations and in the long time limit this density will converge to a normalisable invariant density, for example for the PM map when $\alpha > 1$. However, when $\alpha < 1$ the PM transformation is analyzed with an infinite, i.e. non normalisable, density $\rho_{\text{inf}}(|v|)$ (see Fig. 7). The infinite density is related to the normalized density according to

$$\rho_{\text{inf}}(|v|) \sim t^{1-\alpha} \rho(|v|, t). \quad (70)$$

In fact now it becomes clear that the object on the left hand side is not normalisable, since the integral over $|v|$ of $\rho(|v|, t)$ is unity, and $t^{1-\alpha} \rightarrow \infty$ when $0 < \alpha < 1$. This definition can be used to estimate the infinite density from numerical data (mathematician usually define the

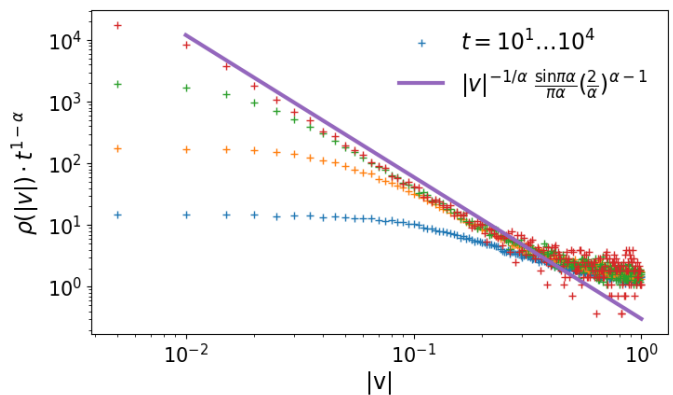


FIG. 7. Infinite invariant density of the Pomeau-Manneville map (also see in Korabel and Barkai [32]) for $z = 3.3$. As described in Eq. (70) the rescaled density approaches Eq. (71). The averaging was done over 10000 trajectories.

infinite density up to a non specified constant, but here we follow convention in [32, 33]). It can be shown that

$$\rho_{\text{inf}}(|v|) = |v|^{-1/\alpha} \frac{\sin \pi \alpha}{\pi \alpha} \left(\frac{\tilde{a}}{\alpha} \right)^{\alpha-1} h(|v|). \quad (71)$$

Here $h(|v|)$ is a bounded function of order of unity, and most importantly $h(0) = 1$. This means that the infinite density has a singularity close to $|v| \rightarrow 0$ namely $\rho_{\text{inf}}(|v|) \sim |v|^{-1/\alpha}$. Consistently for $0 < \alpha < 1$ the infinite density is clearly not integrable. The beauty of infinite ergodic theory is that one may still construct an ergodic theory based on this non-normalized function. Here we must distinguish between observables integrable and non-integrable with respect to the infinite density. In our study we need the second moment of the velocity found using Eq. (70)

$$\langle |v|^2 \rangle = \frac{\int_0^1 |v|^2 \rho_{\text{inf}}(|v|) d|v|}{t^{1-\alpha}}. \quad (72)$$

Using Eq. (71) the integral is finite, meaning that the observable is integrable with respect to the infinite density if $\alpha > 1/3$ or $z < 4$. As long as $2 < z < 4$ we have from Eq. (73) $\beta = \alpha - 1 = (2 - z)/(z - 1)$.

When $z > 4$ the variable $|v|^2$ is non integrable with respect to the infinite density. The average of this observable is then obtained using Thaler-Dynkin limit theorem. Dynkin's result [34] was derived in the context of renewal theory in particular the analysis of the forward recurrence time [22], while Thaler established the connection to the underlying transformations [35]. We will not go into the details since they were recently explained in [36]. Briefly, we define the rescaled variable with $y = |v|(\tilde{a}t)^\alpha/\alpha^\alpha$ and the normalized PDF of $y > 0$, in the long time limit, is $q(y) = [\sin \pi \alpha / \pi \alpha] / [1 + y^{1/\alpha}]$. A numerical calculation is shown in Fig. 8. Averages like $|v|^2$ which is of course proportional to averages of y^2 are now obtained with this limiting PDF. Importantly we have the scaling $|v| \sim t^{-\alpha}$

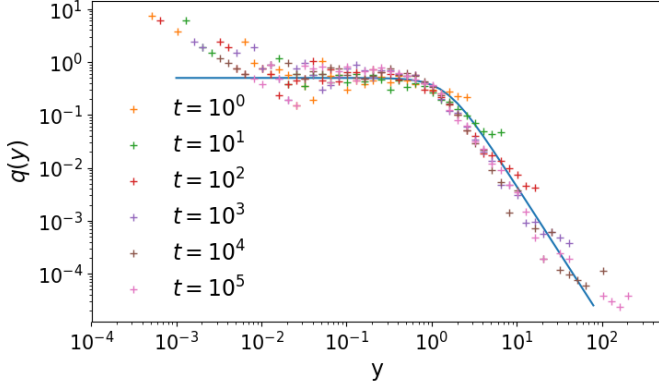


FIG. 8. Thaler-Dynkin limit Theorem for the Pomeau-Manneville map (also see in Akimoto and Barkai [36]) for $z = 3.5$. The rescaled densities of the transformed variable y at different times t (points) collapse to a universal curve described by Eq. (73) (blue curve).

(but this should be used with care, and is limited to the observables non integrable with respect to the infinite density). It is easy to show that

$$\langle |v|^2 \rangle \sim \left(\frac{\alpha}{at} \right)^{2\alpha} \int_0^\infty \frac{\sin \pi\alpha}{\pi\alpha} \frac{y^2}{1 + y^{1/\alpha}} dy. \quad (73)$$

So we have $\beta = -2\alpha = -2/(z-1)$, for $z > 4$, as in Eq. (69). Note that the integral in Eq. (73) blows up when $\alpha > 1/3$, i.e. $z < 4$, due to the upper limit, hence in that case the observable y^2 (or $|v|^2$) is non-integrable with respect to the Thaler-Dynkin distribution. In that sense the infinite density and the Thaler-Dynkin limit theorem are complimentary to one another, in fact large y behavior of the latter matches the small argument behavior of

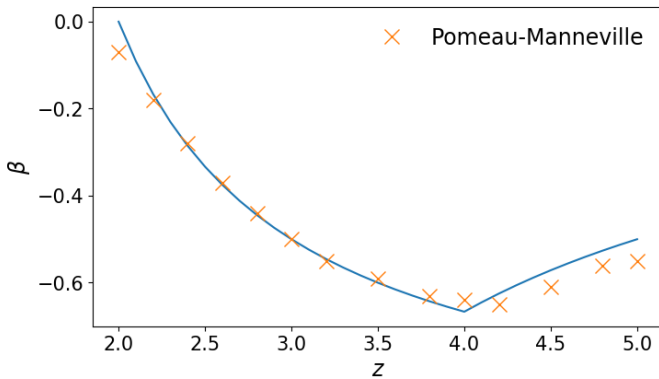


FIG. 9. The scaling β of the velocity displacement $\langle v^2 \rangle$ was fitted after $t = 10^6$ iterations of the map. The solid curve shows the analytical calculation β for $t \rightarrow \infty$ using the infinite invariant density ($z < 4$) and the Thaler-Dynkin limit theorem ($z > 4$) (see Eq. (73)). The exponent beta is negative since the particle is attracted to the unstable fixed points on $v = 0$, so $\langle v^2 \rangle$ is decreasing with time as more particle are accumulated close to the unstable fixed point.

the former, the existence of two limits is related to non uniform convergence of the density of $|v|$. To summarize β in our process is given by

$$\beta = \begin{cases} \nu - 2 = 2\gamma - 2 & \text{if } 2\gamma > 1 + \alpha \\ \alpha - 1 & \text{if } 2\gamma < 1 + \alpha. \end{cases} \quad (74)$$

See Fig. 9 for the numerical calculation. Note that the result is identical to the value of β in Eq. (53). We can also see the exponent β in the velocity correlation function (see Fig. 10). However, we have to be careful about how we make the transition $\tau/t \rightarrow 0$.

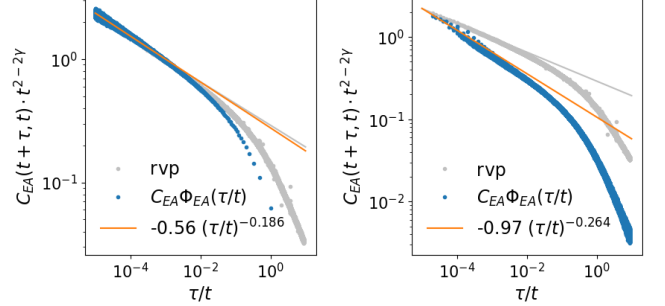


FIG. 10. Calculation of the exponent δ_1 ($\beta = \delta_1 + \nu - 2$) from the velocity correlation function of the Pomeau-Manneville map compared to the data for the renewal velocity process in Fig. 3. Left: Scaling function for $\tau = \text{const} = 10$ and $t \rightarrow \infty$ gives the expected result for β . Right: using the same data as in Fig. 5. The exponent is different from the expected δ_1 and the data for different τ does not collapse close to zero to one curve.

C. Scaling of the time average

Now we have transport exponents. We insert Eq. (74) and (68) in Eq. (21) and get for the TA MSD

$$\langle \overline{\delta^2} \rangle \sim \begin{cases} t^{\frac{2-z}{z-1}} \Delta^3 \left(\frac{z-2}{z-1} \right) & 5/2 < z < 4 \\ t^{-\frac{2}{z-1}} \Delta^2 & z > 4 \end{cases} \quad (75)$$

The exponent of Δ in the TA MSD will now be called η i.e. $\delta^2 \propto \Delta^\eta$. Eq. (75) yields the EA TA MSD. What will one observe based on an individual trajectory analysis without any ensemble averaging? Generating one trajectory at a time using the Pomeau-Manneville map we estimate numerically δ^2 . Fig. 11 shows that the scaling dependence on Δ is stable even if the pre-factors of the TA MSD fluctuate.

For $z > 2.5$ it is identical to $\nu - \beta$. If z is smaller than 2.5 condition (14) does not hold and thus the scaling Green-Kubo relation is not applicable. For $z > 4$ the particle exhibits ballistic behavior as the TA MSD increases quadratically with Δ but also aging as the Δ^2 pre-factor is shrinking as we increase the observation time. This large $4 < z$ limit corresponds to small values of α which

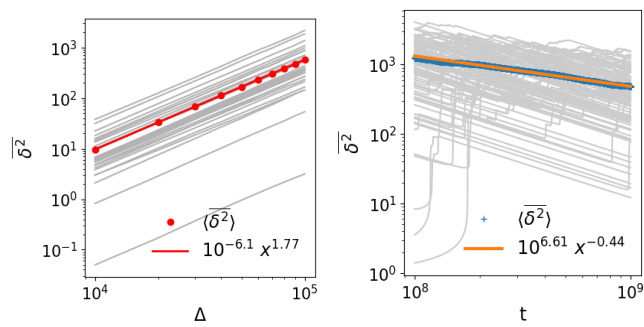


FIG. 11. TA MSD of the deterministic system: Calculation of the dependence on Δ (left) for $z = 3.5$, $t = 10^{10}$ and t (right) for $z = 2.8$, $\Delta = 10^6$. In both panels we present also the EA TA MSD (colored lines) which nicely match with Eq. (75). We see that the scaling with Δ is very stable within the ensemble (grey curves) and fluctuations are only visible in the pre-factor. In contrast for the dependence of δ^2 on t the EA is not similar to one single TA MSD calculation.

means that the particle is getting trapped very close to the vicinity of the two-sided unstable fixed point on the origin, so velocity is effectively decreasing (i.e. $\beta < 0$) but still the particle remains with $v > 0$ or $v < 0$ without switching sign, for times of the order of measurement time, which gives the ballistic like feature of the time averaged MSD. As we cross to the regime $2.5 < z < 4$, α is decreased, the ballistic transport turns super-diffusive, but still we have an aging pre-factor. The results for the scaling are the same that we got for the renewal velocity process (see Fig. 12). The scaling Green-Kubo approach is not valid for $z < 2.5$ since the condition $\nu - \beta > 1$ does not hold there. This does not mean that $z < 2.5$ exhibits perfectly normal diffusion, namely scaling Green-Kubo and standard Green-Kubo relations, are not yet the complete story.

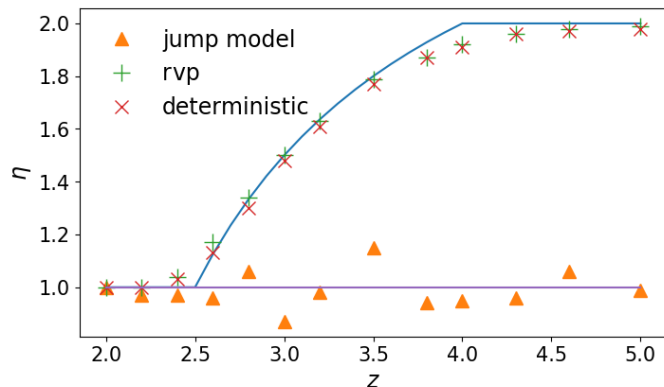


FIG. 12. Scaling exponent in Δ of the TA MSD for all three processes

VII. CONCLUSION

We found a theory that relates the TA MSD to the correlation function if the velocity correlation function is scale invariant and the scaling exponents β and ν obey Eq (14). The scaling GK relation can be applied for systems where the usual Green-Kubo relation does not work. There are several systems where this approach could be useful, like cold atoms diffusivity on optical lattices, active transport in cells and blinking quantum dots [8].

With the scale invariant GK relation we can calculate the TA MSD of renewal velocity processes. Depending on the waiting time distribution and the velocity scaling the process might show either subdiffusion, normal diffusion, superdiffusion or ballistic motion. A transition occurs when $2\gamma = \alpha + 1$. The most simple version of such a renewal velocity process where $v_{\gamma,t} = \pm 1$ can easily be related to a random walk model where jump length and waiting time distribution are the same. We explored cases where the scaling exponents of the EA MSD are identical for the random walk and velocity approach, still the exponents of the TA procedure for the two models differ. This is somewhat surprising as on the renewal times, the path of the two processes is identical. So the TA MSD is sensitive to the choice of the model and to the precise definition of the paths (see Fig. 4). In the context of Langevin equation with multiplicative noise, the difference between Ito and Stratonovich calculus, which is also related to the precise definition of stochastic paths, is well documented [37]. In this manuscript, within the context of anomalous diffusion, the exact shape of the path is also extremely important (unlike normal processes). The effect stems from the fact that in the measurement time interval $(0,t)$ we have a single flight or waiting event that dominates the trajectory, in the sense that these are of the order of measurement time t [38]. Hence, the precise definition of the path of the particle in this interval, crucially influences the output of the time averaged procedure, but not the ensemble average, since the latter is a measure of where is the particle at the moment of observation, while the former a functional of the whole path.

We also investigated a deterministic model of a diffusion process generated by a symmetric version of the Pomeau-Manneville map. Here numerical calculations of the correlation function showed that the exponent δ_1 depends on how the limit $\tau/t \rightarrow 0$ is approached. Analytical calculations can be done using infinite ergodic theory. The result for the scaling exponents is the same as for the stochastic velocity model. In the range where the integration of v^2 with respect to the infinite invariant density diverges, the Thaler-Dynkin law can be applied.

ACKNOWLEDGMENTS

This work was supported by the Israel science foundation.

-
- [1] R. Kubo, *Rep. Prog. Phys.* **29**, 255 (1966).
- [2] R. Metzler, J. H. Jeon, A. G. Cherstvy, and E. Barkai *Phys. Chem. Chem. Phys.* **16**, 24128 - 24164 (2014).
- [3] D. A. Kessler and E. Barkai, *Phys. Rev. Lett.* **105**, 120602 (2010).
- [4] N. Leibovich and E. Barkai, *Phys. Rev. E* **88**, 032107 (2013).
- [5] A. Taloni, A. Checkkin, and J. Klafter, *Phys. Rev. Lett.* **104**, 160602 (2010).
- [6] A. G. Cherstvy, A. V. Checkkin, and R. Metzler, *New J. Phys.* **15**, 083039 (2013).
- [7] G. Margolin and E. Barkai, *J. Chem. Phys.* **121**, 1566 (2004).
- [8] A. Dechant, E. Lutz, D. A. Kessler and E. Barkai *Phys. Rev. X* **4**, 011022 (2014).
- [9] J. Klafter, A. Blumen, and M. F. Shlesinger, *Phys. Rev. A* **35**, 3081 (1987).
- [10] T. Akimoto and T. Miyaguchi *J. Stat. Phys.* **157** 515 (2014).
- [11] T. Albers, Ph.D. diss., TU Chemnitz, 2016.
- [12] V. Zaburdaev, S. Denisov and J. Klafter *Rev. Mod. Phys.* **87** 483 (2015).
- [13] D. Froemberg and E. Barkai *European Physical Journal B* **86**, 331 (2013).
- [14] T. Akimoto, E. Barkai and K. Saito *Phys. Rev. Lett.* **117**, 180602 (2016).
- [15] Y. He, S. Burov, R. Metzler, E. Barkai *Phys. Rev. Lett.* **101**, 058101 (2008). See viewpoint in Igor M. Sokolov, *Physics* 1, 8 (2008).
- [16] C. Beck and G. Roepstorff, *Physica A* **145**,1 (1987)
C. Beck, *Physica A* **233**,419 (1996).
- [17] Y. Pomeau and P. Manneville, *Commun. Math. Phys.* **74**, 189 (1980).
- [18] E. Barkai, *Phys. Rev. Lett.* **90**, 104101 (2003).
- [19] G. Bel and E. Barkai, *EPL* **74**(1), 15 (2007).
- [20] G. Zumofen, and J. Klafter, *Phys. Rev. E* **47**, 851 (1993).
- [21] N. Leibovich, A. Dechant, E. Lutz, and E. Barkai *Phys. Rev. E* **94**, 052130 (2016).
- [22] C. Godrèche and J. M. Luck, *J. of Statistical Physics* **104**, 489 (2001).
- [23] T. Geisel and S. Thomae, *Phys. Rev. Lett.* **52**, 1936 (1984).
- [24] D. Froemberg and E. Barkai *Phys. Rev. E* **87**, 030104(R) (2013).
- [25] J. P. Bouchaud and A. Georges, *Phys. Rep.* **195**, 127 (1990).
- [26] R. Metzler and J. Klafter, *Phys. Rep.* **339**, 1 (2000).
- [27] J.W. Haus, K.W. Kehr, *Phys. Rep.* **150**, 141 (1987)
- [28] M. M. Meerschaert and P. Straka, *Ann. Probab.* **42** (4), 16991723 (2014)
- [29] M. Dentz, T. Le Borgne, D. R. Lester and F. P. J. de Barros, *Physical Review E* **92**, 032128 (2015)
- [30] R. Kutner and J. Masoliver *The European Phys. Journal B* (2017) 90: 50.
- [31] V. Zaburdaev, S. Denisov and J. Klafter, *Rev. Mod. Phys.* **87**, 483 (2015).
- [32] N. Korabel, E. Barkai *Phys. Rev. Lett.* 102, 050601 (2009).
- [33] N. Korabel, and E. Barkai *J. of Statistical Mechanics: Theory and Experiment* (2013) P08010.
- [34] E. Dynkin, in *Selected Translations in Mathematical Statistics and Probability* (American Mathematical Society, Providence, RI, 1961), Vol. 1, pp. 171-189.
- [35] M. Thaler, *Stoch. Dyn.* 5, 425 (2005).
- [36] T. Akimoto and E. Barkai, *Phys. Rev. E* **87**, 032915 (2013).
- [37] C.W. Gardiner *Handbook of Stochastic Methods for Physics, Chemistry and the Natural Sciences*, Springer, Berlin (1983)
- [38] C. Godreche, S. Majumdar and G. Schehr, *J. Stat. Mech.* (2015) P03014